Numerical Modeling of GaAs Solar Cell Performances

M. Abderrezek[1,2], F. Djahli[2], M. Fathi[1], M. Ayad[1]
[1]*UDES, Solar Equipments Development Unit EPST/CDER*
RN11 Bou-Ismail BP. 386, 42415 Tipaza, Algeria
[2]*L.I.S Laboratory, Department of Electronic, Faculty of Technology, Ferhat Abbas University, SETIF, Algeria*
mahfoud_cbi@yahoo.fr

***Abstract*—The process of modeling photovoltaic devices is a tedious task in that it depends heavily on several intrinsic and extrinsic properties of the material. In this paper, numerical solutions are obtained using the Personal Computer 1 Dimension (PC1D) software package in order to improve solar cells performance. The analysis deals with high efficiency GaAs solar cells, in order to search the technological parameters leading to optimal performances of the cells, the effects of the doping level and the thicknesses of the base and emitter layers were also investigated. The optimal fill factor and the conversion efficiency that were obtained are 86.76 % and 25.8 % respectively.**

***Index Terms*—GaAs, solar cell, numerical modeling, PC1D, conversion efficiency.**

I. INTRODUCTION

The solar cell is an electronic component capable of providing energy if properly lighted. Generally, its performances depend on manufacturing conditions and its operating environment. Generally, the compounds used in optoelectronics and solar cells at high efficiency, are essentially alloys of elements from column III and column V in the periodic table of elements. The main semiconductors in III-V namely, GaAs and InP can be alloyed with other materials such as Al and Sb to give ternary compounds such as $Al_xGa_{1-x}As$ and $Ga_xIn_{1-x}P$, or quaternary compounds such as $In_xGa_{1-x}As_yP_{1-y}$. They are formed as thin films to be used in different terrestrial and space applications [1]. GaAs is currently one of the most used semiconductors, so that recent research was directed towards the study of gallium arsenide solar cells due to their interesting features, namely, lower temperature coefficient, higher electron saturation velocity and higher electron mobility compared to silicon solar cells [2].

The modeling of photovoltaic devices is not simple; it depends heavily on several intrinsic optoelectronic properties of the material, such as surface recombination velocity and volume, lifetime of minority carriers, and the doping level which is one of the extrinsic parameters which play an essential role. The involvement of all these parameters complicates the resolution of analytical equations. To overcome this, many simplifications and assumptions are used to obtain simpler analytical solutions.

However, those simplifications hide many internal physical phenomena and therefore make the analytical study of solar cells approximate and less rigorous. On the other hand, the use of numerical solution techniques can provide solutions and results close to the experimental ones and allows using maximum data. The simulation of solar cells, using different simulators is a mean for understanding the behavior of these devices. It permits to see the effect of certain parameters (doping levels in both regions, base thickness and junction depth) on the solar cell characteristics namely the short circuit current (I_{sc}), the open circuit voltage (V_{oc}), the conversion efficiency (η) and the fill factor (FF) [3].

In our case, we used the PC1D simulator (Personal Computer 1 Dimension), which was developed by Paul A. Basauri in 1984 to model semi-conductors, including photovoltaic components [4], [5]. It solves the coupled nonlinear equations that govern the physical phenomena within the device to be studied. This simulator is widely used to model the internal operation of crystalline solar cells [6], [7].

In this paper, we will investigate the behavior of the solar cell with respect to technological parameters such the doping level, the thickness of the base and emitter layers and the recombination speed on the front side of the cell and their role in the optimization of the cell.

II. GaAs SOLAR CELLS MODEL

Schematic drawing of basic structure of a mono-crystal GaAs solar cell is shown in Fig. 1.

It is well known that the efficiency of the GaAs solar cells depends on n+p junction's depth. For an optimal value of this parameter, the solar cell operates more efficiently. This is caused, on the one hand, by a specificity of photon processes taking place within the materials contained in the solar cells, and on the other hand, by the features of their designs[8].

To optimize a solar cell, we used its mathematical model considering an abrupt n+p junction and constant doping levels on each side of the n+p junction [9]. We can suppose

Manuscript received January 8, 2013; accepted June 8, 2013.

that the electric field, outside the depletion layer of the n+-p junction, is equal to zero.

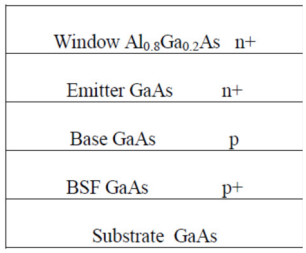

Fig. 1. Basic structure of a GaAs solar cell.

The generation rate of electron-hole pairs at the distance x from the surface is given by the following expression

$$G(x,\lambda) = \alpha(\lambda)\, F(\lambda)\,[1-R(\lambda)]\exp(-\alpha(\lambda)x), \qquad (1)$$

where $\alpha\,(\lambda)$ is the local absorption coefficient, $R\,(\lambda)$ is the surface reflectivity and $F\,(\lambda)$ is the density of photons. For low injection conditions, stationary equations are [5]:

$$(1/q)\,(d\,J_P/dx) - G_P + \Delta p_n/\tau_P = 0, \qquad (2)$$

$$(1/q)\,(d\,J_n/dx) + G_n - \Delta n_P/\tau_n = 0, \qquad (3)$$

$$\Delta P_n = P_n - P_{n0}\ , \quad \Delta n_P = n_P - n_{P0}, \qquad (4)$$

where P_{no} and n_{no} are respectively electrons and holes densities, at the thermodynamic equilibrium and q is the electron charge. J_p and J_p, G_n and G_p, τ_n and τ_p are, respectively, the current densities, the generation rates and the life duration of electrons and holes. The hole and electron densities are given by:

$$J_p = q\,\mu_p\, p_n\, E - q\,D_p\,(dp_n/dx), \qquad (5)$$

$$J_n = q\,\mu_n\, n_p\, E + q\,D_n\,(dn_p/dx), \qquad (6)$$

where E is the electric field and D_p, D_n, μ_p and μ_n are the diffusivity and the mobility of holes and electrons.

The combination of (1), (2) and (5) allows obtaining the following expression describing the distribution of holes in the emitter region (n layer)

$$D_P\frac{d^2\Delta p_n}{dx^2} + \alpha\ F(1-R)\ \exp(-\alpha x) - \frac{\Delta p_n}{\tau_p} = 0. \qquad (7)$$

A similar integro-differential equation for the electron distribution in the p layer can be written as

$$D_n\frac{d^2\Delta n_p}{dx^2} + \alpha\ F(1-R)\ \exp(-\alpha x) - \frac{\Delta n_p}{\tau_n} = 0. \qquad (8)$$

Since (7) and (8) don't have analytical solutions, we used a numerical method with the following initial conditions:

1) At the surface level, the recombination takes place at a speed S_p:

$$D_p\ \frac{d\,\Delta p_n}{dx} = S_p\ \Delta p_n\ \text{at}\ x = 0\,, \qquad (9)$$

$$p_n - p_{n0} = 0\ \text{at}\ x = x_j\,, \qquad (10)$$

where S_p is the surface recombination velocity of holes.

2) In the junction limit, the density of carriers in excess is cancelled by the electric field in the depletion region:

$$-D_p\ \frac{d\,\Delta n_p}{dx} = S_n\ \Delta n_p\ \ \text{at}\ x = H\,, \qquad (11)$$

$$n_p - n_{p0} = 0\ \ \text{at}\ x = x_j + w\,, \qquad (12)$$

where x_j is the junction depth, H is the thickness of the cell, S_n is the back surface recombination velocity of electrons and w is the space charge width. The photo-generated excess hole density in the n region is given by

$$J_p = -qD_p\left(\frac{dp_n}{dx_j}\right) = \left[q\,F(1-R)\ \alpha\ L_p/(\alpha^2 L_p^2 - 1)\right]\times$$
$$\times\left[\frac{\left(\frac{S_p L_p}{D_p} + \alpha L_p\right) - \exp(-\alpha x_j)\left(\frac{S_p L_p}{D_p}\cosh\frac{x_j}{L_p} + \sinh\frac{x_j}{L_p}\right)}{\frac{S_p L_p}{D_p}\sinh\frac{x_j}{L_p} + \cosh\frac{x_j}{L_p}} - \alpha L_p \exp(-\alpha x_j)\right]. \qquad (12)$$

While the photo-generated excess hole density in the p region is given by

$$J_n = \frac{qF(1-R)\alpha L_n}{\left(\alpha^2 L_n^2 - 1\right)}\exp\left[-\alpha(x_j + w)\right]\times$$
$$\times\left[\alpha L_n - \frac{\left(\frac{S_n L_n}{D_n}\right)\left(\cosh\left(\frac{d'}{L_n}\right) - \exp(-\alpha d')\right) + \sinh\left(\frac{d'}{L_n}\right) + \alpha\ L_n\ \exp(-\alpha d')}{\frac{S_n L_n}{D_n}\sinh\left(\frac{d'}{L_n}\right) + \cosh\left(\frac{d'}{L_n}\right)}\right], \qquad (13)$$

where d' is width of base and L_P and L_n are hole and electron diffusion lengths.

The total photo-current as a function of the wavelength is defined as the sum of diffusion currents in the *p-*, *n-* regions and depletion region [5]

$$J_E(\lambda) = J_p(\lambda) + J_n(\lambda) + J_{dr}(\lambda), \qquad (14)$$

where

$$J_{dr} = qF(1-R)\exp(-\alpha x_j)\left[1 - \exp(-\alpha w)\right]. \qquad (15)$$

The most important Semiconductor parameter is the conversion efficiency η, given by

$$\eta = P_m / P_{in} = FFV_{oc}J_{sc} / P_{in}\,, \qquad (16)$$

where $P_m = I_m\ V_m$ is the maximum output power of SC, P_{in} is the integral solar incident power on the front contact, V_{oc} is the open circuit voltage, J_{sc} is the short circuit current density and FF is the Fill factor which determines the SC losses.

III. Results and Discussion

The choice of the optimal parameters of each area of the cell was carried out in order to attain the best compromises

between the conversion efficiency η and the Fill factor FF. To study the influence of the base parameters, we varied the thickness of the latter between 1 µm and 9 µm and its doping level between 1×10^{16} cm^{-3} and 2×10^{18} cm^{-3}. Moreover, the parameters chosen for the emitter, the BSF (back surface field) layer and the window layer are respectively: $N_D = 2 \times 10^{18}$ cm^{-3} and $X_E = 0.05$ µm, $N_A = 2 \times 10^{18}$ cm^{-3} and $X_{BSF} = 0.5$ µm, $N_D = 2 \times 10^{18}$ cm-3, $X_{window} = 0.05$ µm. Details about the main parameters of the semiconductors used in our simulation are summarized in Table I.

TABLE I. MAIN PARAMETERS USED IN THE SIMULATION.

Material	GaAs	$Al_{0.8}Ga_{0.2}As$
Band Gap(eV)	1.42 [10]	2.09 [11]
Electron affinity (eV)	4.07 [10]	3.53 [11]
Dielectric permittivity(relative)	13.18 [10]	10.68 [11]
Eelectron mobility (cm²/Vs)	Varied [12]	212 [13]
Hole mobility (cm²/Vs)	Varied [12]	67 [13]
Radiative recombination coefficient (cm³/s)	7.20E-10 [10]	7.50E-10 [11]
Lattice constant a(A°)	5.65 [10]	5.64 [13]
Absorption coefficient	Data from [14]	Data from [11]

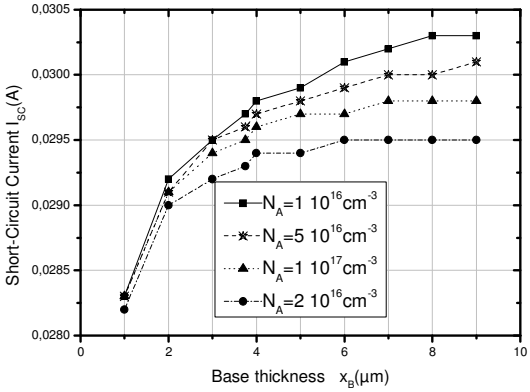

Fig. 2. Base parameter effect on the short-circuit current of the GaAs cell.

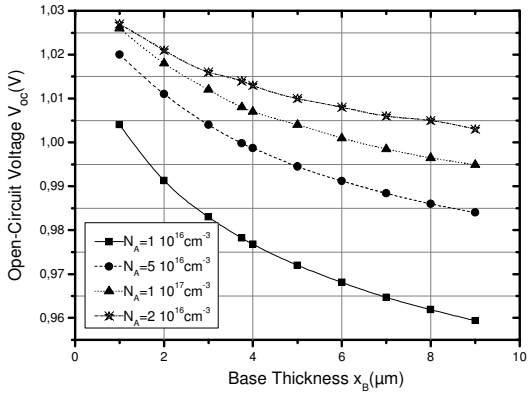

Fig. 3. Base parameter effect on the open circuit voltage of the GaAs cell.

Results of PC1D simulation (using these assumptions) are shown in Fig. 2, one can see that the short-circuit current is proportional to the thickness of the base. The variation is very fast until $X_E = 4$ µm, then it starts to stabilize around a constant value. Considering the good absorption properties of GaAs, this thickness is sufficient to exploit a broad range of the solar spectrum. However, the same figure shows that the current is inversely proportional to the doping of the base. This degradation of the current is due to the higher doping level which decreases the resistivity of the base. The phenomenon is reversed with the open circuit voltage; the voltage increases with the doping and decreases with the thickness (Fig. 3). We note, moreover, that the best conversion efficiency of the cell (η =25.8%), is obtained for a base doping $N_A=1\times10^{17}$cm^{-3} and a thickness $X_B=3.75$ µm (Fig. 4).

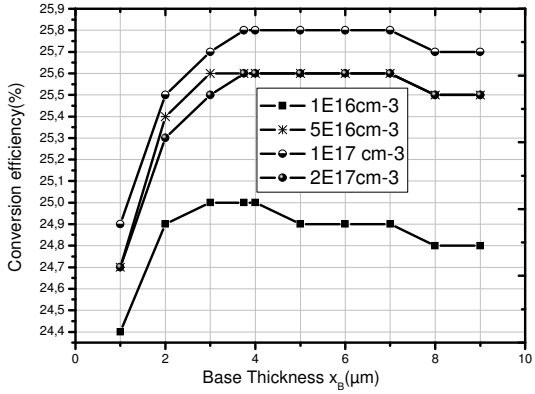

Fig. 4. Base parameter effect on the conversion efficiency of the GaAs cell.

The spectral response is degraded when the doping of the emitter increases. It reaches its maximum value (> 95 %), in the wavelengths range of 300 nm–800 nm (Fig. 5.)

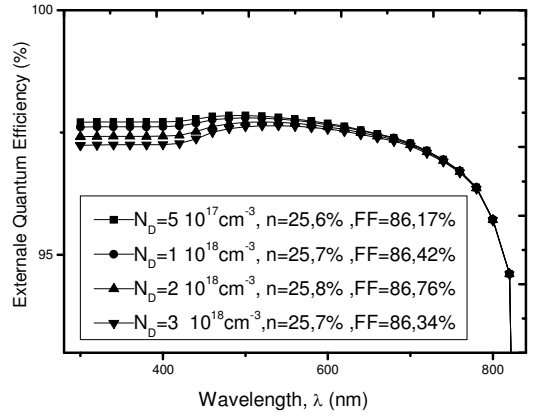

Fig. 5. Emitter parameter effect on the spectral response of the GaAs cell.

Good results were obtained for an emitter thickness $X_E = 0.05$ µm and a doping $N_D = 2 \times 10^{18}$ cm^{-3} (Fig. 6). The best obtained results are η = 25.8 % and FF = 86.76 %.

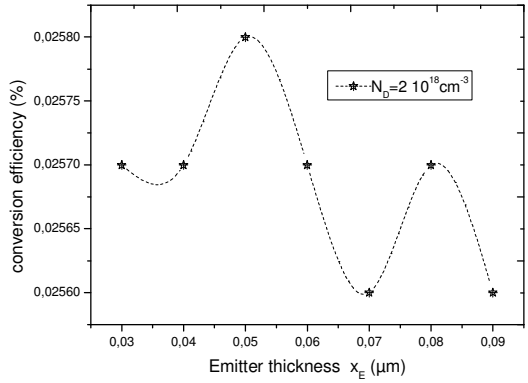

Fig. 6. Emitter thickness effect on the conversion efficiency of the GaAs cell.

A high recombination speed, on the front surface, strongly degrades the performances of the solar cell, because the carriers created by the short wavelengths recombine

before reaching the junction. The effect of this phenomenon on the cell quantum efficiency is illustrated in Fig. 7.

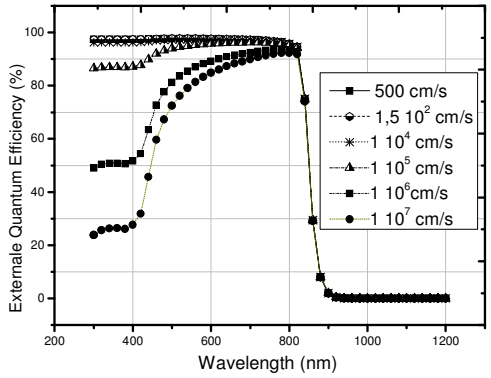

Fig. 7. Effect of the front surface recombination speed on the spectral response of the GaAs cell.

Figure 8 presents the I (V) and P (V) characteristics of the GaAs solar cell optimized.

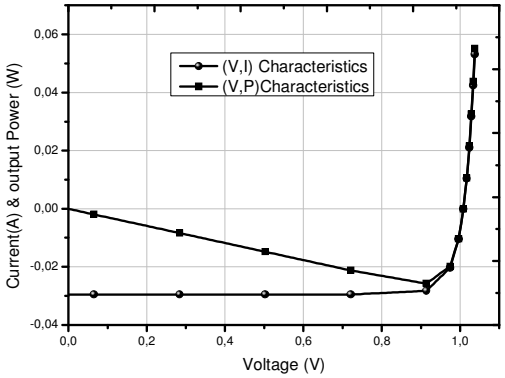

Fig. 8. I (V) and P (V) Characteristics of the GaAs solar cell.

IV. CONCLUSIONS

Considering the results obtained on the GaAs solar cell, we can note that the best results (for η and FF) were obtained for a base layer thickness of X_B = 3.75 µm and a doping level of $N_A = 1 \times 10^{17}$ cm^{-3}. Notice also that to improve, simultaneously, the electric characteristics and the spectral response of the cell; it is necessary to make a compromise between the emitter thickness and its doping level.

Furthermore, the use of the thin window layer (having a low recombination speed) improves the spectral response. In addition to the optimal values of X_B and N_A, given in point (1) for the base layer, the chosen parameters were $N_D = 2 \times 10^{18}$ cm-3 and X_E = 0.05 µm for the emitter layer, and $N_A = 2 \times 10^{18}$ cm^{-3} and X_{BSF} = 0.5 µm for the BSF layer. The output characteristics of the GaAs solar cell were: I_{SC} = 0.0295 A, V_{OC} = 1.008 V, η = 25.8 % and FF = 86.76 %.

Finally, in order to improve the solar cell performances, especially the conversion efficiency, we plan in future works, the use of new materials type PMMA (Polymer Material of Polymethyl Methacrylate) doped with optically active molecules (dyes) like encapsulation materials in design of GaAs solar cells. These allow shifting the solar spectrum from the ultraviolet region where the quantum efficiency (QE) of the cell is poor to the visible region where the QE is higher to the visible region where the QE is higher.

ACKNOWLEDGMENT

The authors would like to express their acknowledgement and gratitude to Dr Paul A. Basore Photovoltaics special research centre, University of New South Wales, for the PC1D program.

REFERENCES

[1] A. F. Meftah , N. Sengouga , A.M. Meftah , S. Khelifi, "Numerical simulation of the effect of the Al molar fraction and thickness of an $Al_xGa_{1-x}As$ window on the sensitivity of p^+-n-n^+ GaAs solar cell to1 MeV electron irradiation", *Renewable Energy,* no. 34, pp. 2426–2431, 2009. [Online]. Available: http://dx.doi.org/10.1016/j.renene. 2009.03.013

[2] A. Luque, S. Hegedus, *Handbook of Photovoltaic Science and Engineering*. New Jersey USA: John Wiley & Sons, Hoboken, 2003, pp. 360–411. [Online]. Available: http://dx.doi.org/10.1002/ 0470014008

[3] M. Zeman, J. Krc, "Electrical and Optical Modelling of Thin-Film Silicon Solar Cells", *Journal of materials research*, no. 4, vol. 23, pp. 889–898, Apr. 2008.

[4] D. Clugston, P. Basore, "PC1D Version 5: 32-bit Solar Cell Modeling on Personal Computers", in *Conf. Rec., 26th IEEE Photovoltaic Specialists*, Anaheim CA, 1997, pp. 207–210.

[5] M. Burgelman, J. Verschraegen, S. Degrave, P. Nollet, "Modeling Thin-film PV Devices", *Prog. Photovolt: Res. Appl*., no. 12, pp. 143–153, 2004. [Online]. Available: http://dx.doi.org/10.1002/pip.524

[6] R. Brendel, "Modeling solar cells with the dopant-diffused layers treated as conductive boundaries", *Progress in Photovoltaics Research and Applications*, pp. 31–43, Jan. 2012, [Online]. Available: DOI: 10.1002/pip.954

[7] C. Vázquez, J. Alonso, M. A. Vázquez, L. J. Caballero, R. Romero, J. R. Ramos-Barrado, "Efficiency of commercial Cz-Si solar cell with a shallow emitter", *Materials Science and Engineering: B*, vol. 172, no. 1, pp. 43–49, Aug. 2010. [Online]. Available: http://dx.doi.org/ 10.1016/j.mseb.2010.04.015

[8] R. Anil Kumar, M. S. Suresh, J. Nagaraju, *Solar energy Materials & solar cells*, 2003, pp. 145–153. [Online]. Available: http://dx.doi.org/10.1016/S0927-0248(02)00316-1

[9] A. Goetzberger, J. Knobloch, B. Vo, β *Crystalline Silicon Solar Cells*, John Wiley & Sons, 1998, pp. 67–75.

[10] K. J. Singh, S. K. Sarkar, "Highly efficient ARC less InGaP/GaAs DJ solar cell numerical modeling using optimized InAlGaP BSF layers", *Springer Opt. Quant Electron*, vol. 43, no. 1–5, pp. 1–21, 2011.

[11] S. Adachi, "GaAs, AlAs and $Al_xGa_{1-x}As$, material parameters for use in research and device applications", *Journal of Applied Physics*, vol. 58, no. 3, pp. 1–29, 1985. [Online]. Available: http://dx.doi.org/ 10.1063/1.336070

[12] M. Y. Ghannam, A. S. Alomar, N. Posthuma, G. Flammad, J. Poorthmans, "Optimization of the triple junction In0.5Ga0.5P/GaAs/Ge monolithic tandem cell aimed for terrestrial using an experimentally verified analytical model", *Kwait J. Sci*. vol. 31, no. 2, pp. 203–234, 2004.

[13] *New Semiconductor Materials. Characteristics and Properties*. [Online]. Available: http://www.ioffe.ru/SVA.

[14] S. Adachi, *Optical Constants of Crystalline and Amorphous Semiconductors - Numerical Data and Graphical Information*, Springer – Verlag, 1999, pp. 220–226.